LBL-19325
Preprint c.2

Lawrence Berkeley Laboratory
UNIVERSITY OF CALIFORNIA

Materials & Molecular Research Division

LAWRENCE
BERKELEY LABORATORY
1986
LIBRARY AND

Submitted to Physical Review B

A GENERALIZED RAMSAUER-TOWNSEND RESONANCE IN ARPEFS OSCILLATIONS

J.J. Barton, Z. Hussain, and D.A. Shirley

April 1986

TWO-WEEK LOAN COPY
This is a Library Circulating Copy
which may be borrowed for two weeks.

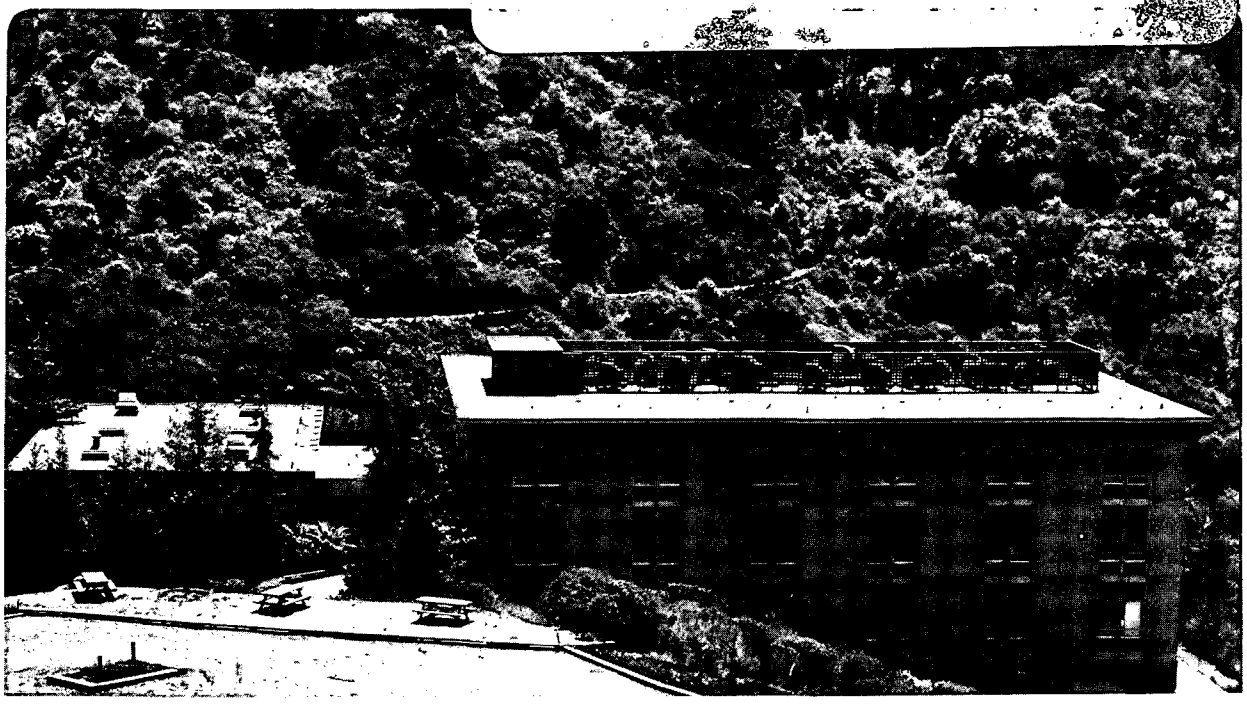

LBL-19325 c.2

Prepared for the U.S. Department of Energy under Contract DE-AC03-76SF00098

DISCLAIMER

This document was prepared as an account of work sponsored by the United States Government. While this document is believed to contain correct information, neither the United States Government nor any agency thereof, nor the Regents of the University of California, nor any of their employees, makes any warranty, express or implied, or assumes any legal responsibility for the accuracy, completeness, or usefulness of any information, apparatus, product, or process disclosed, or represents that its use would not infringe privately owned rights. Reference herein to any specific commercial product, process, or service by its trade name, trademark, manufacturer, or otherwise, does not necessarily constitute or imply its endorsement, recommendation, or favoring by the United States Government or any agency thereof, or the Regents of the University of California. The views and opinions of authors expressed herein do not necessarily state or reflect those of the United States Government or any agency thereof or the Regents of the University of California.

LBL-19325

A GENERALIZED RAMSAUER-TOWNSEND RESONANCE IN ARPEFS OSCILLATIONS

J.J. Barton, Z. Hussain,* and D.A. Shirley

Materials and Molecular Research Division
Lawrence Berkeley Laboratory
and
Department of Chemistry
University of California
Berkeley, California 94720

ABSTRACT

We observe a resonance in the scattering amplitude for S(1s) photoelectrons from Ni atoms and interpret this resonance as a dip in the Ni atom partial cross section for electron scattering related to the Ramsauer-Townsend effect. This generalized Ramsauer-Townsend effect occurs at a particular energy and angle rather than in the total elastic cross section. We show that the resonance energy is sensitive to curved-wave corrections and, after including multiple-scattering effects, we derive the S-Ni bond length in c(2x2)S/Ni(100) from the ARPEFS oscillations arising from the scattering of S(1s) photoelectrons off of nearest neighbor Ni atoms in the presence of the generalized Ramsauer-Townsend resonance. We find this bond length to be 2.20 Å ± .03 Å corresponding to a S-Ni interplanar distance ($d_\perp$) of 1.32 ± .04 Å.

---

*Department of Physics, University of Petroleum & Minerals, Dhahran, Saudi Arabia.

I. INTRODUCTION

The nature of the core-level photoemission intensity oscillations known as photoelectron diffraction has been substantially clarified by new theoretical[1,2] and experimental work which shows that these oscillations--caused by interference between direct and scattered photoemission probability amplitude[3,4]--are qualitatively predicted by scattering path-length differences. A complete understanding of the physics of these oscillations has important consequences for the use of photoelectron diffraction as a technique for determining surface structure: the total scattering path-length difference is the sum of a geometrical path length and an ion-core potential phase shift function of the scattering atom, allowing the geometry to be deduced if the potential can be adequately modeled. While most of the energy dependent photoelectron diffraction measurements[5,6] have been made in the kinetic energy range from 20-150 eV, we have recently[7,8] been concentrating on photoelectron energies between 100-600 eV. These intermediate energies and the wider energy range are advantageous if we wish to concentrate on structure determination because the potential phase shift functions are less sensitive to chemical effects, the photoabsorption cross section has less structure, and the photoelectron scattering partial cross section is more anisotropic giving a simpler and more structure sensitive spectrum. For very similar reasons the x-ray absorption fine structure spectroscopies have been divided into x-ray absorption near edge structure (XANES or NEXAFS) at low energies and extended x-ray absorption fine structure (EXAFS) in the intermediate 100-1000 eV range. We refer to the core-level angle-resolved photoemission measurements in

the 100-1000 eV, intermediate energy range as angle-resolved photoemission extended fine structure (ARPEFS).

To concentrate on the oscillating, non-atomic signal we remove the slowly varying part, I_0, of the intensity, I, to form $\chi = (I-I_0)/I_0$. Every model for ARPEFS predicts that the oscillations, expressed as a function of electron wave number, k, are cosinusoidal:

$$\chi(k) = \sum_j A_j(k) \cos [kr_j(1 - \cos \theta_j) + \phi_j(k)]$$

where $A_j(k)$ is an amplitude function, ϕ_j is a scattering potential phase function, and $(r_j - r_j \cos \theta_j)$ is the geometrical path-length difference for bond length r_j and scattering angle θ_j. The sum on j extends over all atoms near the photoemitter which have significant amplitude. In the simplest case, the amplitude function is large for only a few atoms and has little structure as a function of k, and the phase similarly benign. Then the ARPEFS curve may be Fourier analyzed and--provided Fourier resolution is adequate--the Fourier amplitude spectrum should have peaks corresponding to scattering path-length differences.[7] If, on the other hand, the amplitude function is not a smooth envelope, the Fourier spectrum for the corresponding scattering event will not peak at the scattering path-length difference. In this paper we investigate structure determination with ARPEFS in the case that the scattering potential for nearest neighbor scattering atom has a strong amplitude dependence caused by an interesting resonance related to the Ramsauer-Townsend effect.

We have selected c(2x2)S/Ni(100) for our study primarily because the S adsorption site and the S/Ni bond length have been reported

previously and the overlayer can be reproduced easily. Elsewhere we report[9] a study of the S(1s) ARPEFS from c(2x2)S/Ni(100), concentrating on the scattering events which have Fourier peaks near the scattering path-length difference. Here we will discuss normal emission S(1s) ARPEFS from the nearest neighbor Ni atoms in the four-fold hollow site. The amplitude for the scattering of S photoelectrons from Ni potentials into the normal direction dips sharply as the energy is scanned leading to a split Fourier peak.

II. EXPERIMENTAL

We have given a thorough discussion of our measurement procedure in ref. 9 so we will be brief here. Our sample was prepared in a standard fashion: a mirror-finish, oriented Ni(001) single crystal was cleaned in vacuum, exposed to $H_2S(g)$, and heated briefly to 200°C to give a very sharp c(2x2)S/Ni(100) LEED pattern. This sample was illuminated by soft x-rays from the Stanford Synchrotron Radiation Laboratory Jumbo monochromator[10] and S(1s) angle-resolved photoemission intensity spectra were measured every 3 eV for photon energies between 2532 and 2950 eV. Assuming that the x-rays are completely polarized in the plane of the synchrotron storage ring, we oriented the Ni crystal to place the electric vector of the light, $\hat{\varepsilon}$, 30° from the surface normal toward a [110] direction and rotated the angle-resolved electron energy analyzer to collect spectra along the surface normal. The individual photoemission measurements were reduced to partial cross-section measurements in the fashion described in ref. 9.

The resulting ARPEFS curve $\chi(k)$ is given in Fig. 1. The energy scale has been converted to a wavenumber scale using an inner potential of +10.5 eV. The curve is seen to be dominated by an oscillation with ~ 6 cycles in 2π $Å^{-1}$, corresponding to an interference path length of 6 Å. Since we know the nearest neighbor bond length in this system is ~ 2.2 Å corresponding to a maximum path-length difference of 4.4 Å, we can conclude that the nearest neighbor scattering does not dominate this curve.

Fourier transforms of this curve are shown in Fig. 2. For the lower panel, Fig. 2a, we have multiplied $k\chi(k)$ by a Gaussian of full width half maximum of 4 $Å^{-1}$ centered on the data range, added zeroes to

fill 2048 cells and applied the fast Fourier transform; the Fourier transform magnitude is plotted versus path-length difference. In the upper panel the autoregressive Fourier method described in ref 11 has been applied to $k\chi(k)$ and the resulting extrapolated sequence has been multiplied by a Gaussian of 12 $Å^{-1}$ full width half maximum.

The peaks in the Fourier spectrum above 5 Å path-length difference have been discussed in ref. 9. The path-length difference derived from the positions of these Fourier peaks is approximately equal to the scattering path-length difference for backscattering Ni atoms in the second and third Ni layers. The positions of the two peaks below 5 Å do not correspond to any path-length difference, and no feature in the Fourier spectrum appears near 3.5 Å where we would expect a scattering path-length due to Ni nearest neighbors (assuming a four-fold hollow adsorption and reasonable S-Ni bond distances). The physical origin of these peaks is the subject of this paper.

III. GENERALIZED RAMSAUER TOWNSEND RESONANCE

The lack of correspondence between the scattering path-length difference for nearest neighbor Ni atoms and Fourier spectrum peaks is caused by a strong dip in the scattering power for Ni as a function of energy which occurs for scattering angles near those appropriate for normal emission from c(2x2)S/Ni(001). This dip is related to the well-known Ramsauer-Townsend electron scattering resonance,[12] and hence we call this amplitude effect a generalized Ramsauer-Townsend (GRT) resonance.

Ramsauer and Townsend observed that argon becomes transparent to electrons at 0.7 eV. The origin of this surprising lack of scattering, suggested by N. Böhr and verified by Faxen and Holtsmark,[12] follows from the partial-wave formula for the (complex) scattering amplitude for electrons:

$$f(\theta,k) = \frac{1}{2ik} \sum_{\ell=0} (2\ell+1)P_\ell(\cos\theta)(e^{2i\delta_\ell}-1)$$

where $\delta_\ell(k)$ are the ion-core partial-wave phase shifts. At very low kinetic energies only δ_0, the isotropic s wave, contributes to the scattered wave. If, as is the case for Ar at 0.7 eV, the value of the s phase shift was exactly 180°, then even this term goes to zero and the amplitude, $f(\theta,k)$ becomes very small for all angles.

Our generalized Ramsauer-Townsend effect is more complicated.[13] At higher energies many partial waves contribute to the scattering amplitude. Then only with the proper linear combination of angular factors, $(2\ell+1)\ P_\ell(\cos\theta)$, and energy factors, $(e^{2i\delta_\ell}-1)$, will the

scattering amplitude be zero. Thus while the classical Ramsauer-Townsend effect gives zero amplitude at all angles and very low energy based on special behavior by one phase shift, our generalized Ramsauer-Townsend effect occurs at special angles and energies with many phase shifts involved.

Some ideas about the consequences of this effect can be derived from Fig. 3. Scattering amplitudes for four different angles are plotted in the complex plane. For each angle a line represents $f(k,\theta_j)$ for $k = 4\ \text{Å}^{-1}$ (60 eV) to $k = 12\ \text{Å}^{-1}$ (550 eV). The distance from the origin to a point on the line represents the scattering power for that angle and energy; the angle from the positive real axis to that point gives the wave phase shift caused by the potential.

For $\theta_j = 180°$ we see the scattering power peaks broadly around $k = 6\ \text{Å}^{-1}$. From $k = 4\ \text{Å}^{-1}$ to $k = 12\ \text{Å}^{-1}$ the phase angle sweeps gently through ~ 60°. For $\theta_j = 130°$, however, the behavior is radically different. Now the scattering amplitude approaches the origin for $k = 8\ \text{Å}^{-1}$. The amplitude falls nearly to zero here, and the phase angle sweeps rapidly through 180°. The behavior for $\theta_j = 125°$ is similar, but the phase angle is rotating in the opposite direction.

Clear evidence that the generalized Ramsauer-Townsend effect is responsible for splitting the Fourier peak expected near 3.5Å into the two peaks actually observed in the Fourier spectrum is obtained by backtransforming just those Fourier coefficients whose frequencies are less than 5 Å. As shown in Fig. 4, the resulting filtered ARPEFS curve shows a beat pattern consistent with a 3.5Å oscillation with a superimposed amplitude envelope which dips at $k = 7.5\ \text{Å}^{-1}$. If the phase shift function is extracted from the filtered data,[14] it exhibits the

phase jump of π characteristic of the GRT zero crossing as shown in Fig. 5.

In our initial attempts to use the Ni GRT resonance,[15] we sought to compare the observed phase jump to calculated Ni atom phase shift functions. As is evident from a comparison of the experimental phase function to the theoretical phase function calculated in the plane-wave approximation (see Fig. 5, long dashed curve), the resonance position in energy and angle is not correctly placed in this simple model. We therefore introduced curved wavefront corrections[16] which, as the remaining curves in Fig. 5 demonstrate, places the calculated resonance of the experimentally observed energy. That the resonance is sensitive to the wavefunction calculation is not surprising given that several large partial-wave amplitudes must sum to zero at resonance: any slight error in the weighting of these waves will shift the resonance position.

It would appear from Fig. 5 that we may assign the S-Ni bond length by comparing the observed phase shift function shape to calculated functions which include the curved-wave corrections. The strong dependence of the GRT resonance on scattering angle would set a firm limit on the bond distance, and we would have an elegant method to estimate the surface bond angle.[8] However, this does not allow for the possibility of multiple scattering, and in view of the sensitivity of the resonance we must include this effect.

Fortunately, the calculation we require is very modest: we need only 20 scattering paths. The first four are the single scattering paths from the four Ni nearest the photoemitting S, with path lengths near 3.5 A. The single-scattering wave from the nearest neighbors can double scatter from either of two atoms in the S layer, giving a total

of eight more paths near 4.4 Å. We also include scattering from four S atoms at 3.52 Å and four more at 4.98 Å even though the signal from these atoms is very small. Indeed, without curved-wave corrections[16] these S atoms would cancel in pairs: the phase of the direct wave incident upon one member of the pair is opposite the phase for the other. Of the 20 possible paths possible, only ten are unique, and by employing the method of ref 2, the calculation requires no more effort than other steps in the data analysis process.

The resulting multiple-scattering phase functions are shown in Fig. 6. The multiple-scattering effect is small, but it is adding to a near zero signal. We find that the GRT resonance has been pushed up in angle from 127.5° in single scattering to 131° in multiple scattering. Fig. 6 shows that the phase jump for 131.4° is on the opposite side of the origin from the experimental jump, setting an upper bound on the S-Ni interlayer spacing, $d_\perp$ of 1.50Å corresponding to 130.4°. Although this bound is not very useful, we can limit the value of $d_\perp$ much more closely by comparing the experimental phase functions to the multiple-scattering phase functions in Fig. 6. In each comparison, the same geometrical path-length difference has been subtracted from both theory and experiment. The closest match is clearly for 126.5° corresponding to $d_\perp$ = 1.30Å. Because the angles 125.4° and 127.5° correspond respectively to $d_\perp$ = 1.25 Å and $d_\perp$ = 1.35 Å, this comparison alone has the precision to set small error limits on $d_\perp$ (perhaps ± 0.02 - 0.03 Å).

We can also arrive at this conclusion by comparing the ARPEFS oscillations directly. Fig. 7 compares the filtered experimental data to theory curves for S/Ni bond lengths of 2.16 Å ($d_\perp$ = 1.25 Å), 2.19 Å ($d_\perp$ = 1.30 Å) and 2.22 Å ($d_\perp$ = 1.35 Å). Visual comparison is

sufficient to exclude the two extreme geometries. Using the residual, an unweighted sum of the squared differences between experiment and theory, as a measure of the errors, we find a curve of error versus bond length whose minimum lies at 2.20 Å ($d_{\perp}$ = 1.32 Å) as shown in Fig. 8. The theoretical curves were first scaled to the experiment to minimize their residual before constructing the curve of errors to reduce the influence of amplitude factors.

This preference for 2.20 Å bond length is not dependent on the inner potential: the same geometry is found even if both theory and experiment are placed on the experimental energy scale and the inner potential of the theory is allowed to vary. The curve of errors is less sensitive to the structure in this case as can be seen in Fig. 8 because the shift in E_0 partly compensates for an incorrect geometry. At the minimum residual, we find an inner potential of +11 eV, in good agreement with our original selection of +10.5 eV.

IV. DISCUSSION

Our measurement gives 2.20 Å for the S-Ni bond length in c(2x2)S/Ni(001), in good agreement with previous studies.[9] In estimating the precision of our determination we note that the structure information is carried in medium frequency oscillations superimposed upon a smoothly varying signal, and that we have sampled this signal at a much higher frequency than is relevant for the structure analysis. Furthermore we have measured the oscillations over a wide enough energy range to insure that errors in our reduction of the photoemission measurements to oscillations are minimal. The normal emission geometry is technically simpler to align and any small angular errors in the emission direction are self cancelling in the sense that among the four nearest neighbor Ni atoms every scattering path which lengthens with angle has a mate which shortens. We have varied the shape of the I_0 estimate by altering the stiffness of the numerical spline used to derived I_0 from the data without altering the backtransformed oscillations; the autoregressive Fourier transform is not essential for our analysis and the same results may be derived with conventional Fourier methods. A more complete discussion of possible errors may be found in ref 9. We believe our experimental precision is less than ± 0.02 Å.

The accuracy of our bond length is unfortunately not entirely determined by experiment. Even though the Fourier filtering approach we have used here sufficiently restricts the theory problem so that we need not be concerned about convergence in multiple scattering order or curved wave corrections, our result still relies on accurate theoretical curves. By concentrating primarily on the frequency of the

oscillations, our bond length is not sensitive to amplitude factors like inelastic mean free path, thermal averaging, or aperture integration. Furthermore, since the contribution of the path-length difference to the frequency is 20 times larger than the Ni potential phase shift and multiple scattering corrections, even moderate errors in the theoretical contributions to the frequency will not disturb the bond length analysis. More serious sources of error in our procedure are the constant part of the multiple scattering phase shift function and the inner potential, E_0. Either of these parameters will lead to geometry errors as the phase offset of theory and experiment is partial compensated by an erroneous shift in the theory path-length difference. Both the comparison of the curves in Fig. 7 and our residual analysis with variable E_0 in Fig. 8 argue that we have made no large error due to constant phase shift or inner potential here. Altogether we estimate our accuracy as ± 0.02 Å in bond length or ± 0.03 Å in the S-Ni interplanar spacing.

The theory errors are likely to be systematic, but we nevertheless quote our structure as S-Ni bond length of 2.20 Å ± .03 Å ($d_\perp$ = 1.32 ± .04 Å). With additional study of the scattering potential for Ni and S, including the photoion core potential, and additional measurements to insure experimental reproducibility, the accuracy of this type of structure measurement should improve by about a factor of two. We strongly emphasize that accurate structure work with extended fine structure requires a wide energy range. A short energy range is subject to error from construction of the $\chi(k)$ curve to Fourier analysis to theory comparison: the additional data points in an extended range

set the trends of the low frequencies and hence they provide more than a simple statistical improvement in our experiment.

Sagurton, Bullock, and Fadley have recently[17] studied the GRT resonance using single-scattering theory, and they have concluded that the split Fourier peaks characteristic of the GRT resonance cannot be used for quantitative structural analyses. We believe that our work here demonstrates that this is not true, and rather than a serious liability, the GRT resonance has some interesting properties of its own A more difficult problem is the contribution of double scattering to the frequency range occupied by the resonance, scattering which was omitted in the study of Sagurton et al. We have shown here that this problem can be overcome by applying the method of ref 2.

Our goal in this study has been to study the surface geometry and the generalized Ramsauer Townsend resonance ultimately plays only a small role in our work. Understanding the GRT resonance is of course essential, but the presence of the resonance is a hindrance in the sense that the phase jump on resonance is sensitive to non-structural parameters. A minor benefit of the resonance is the relatively flat (k independent) nature of the Ni phase function above and below the resonance with a consequent negligible contribution to the oscillation frequency. We might imagine that the resonance itself could contribute to either the structure study in other surface systems or the study of surfaces in other ways. For example, first row adsorbates would scatter so little that direct comparison of the experimental phase function with the theory phase functions for various scattering angle might be sufficient to extract the structure. More intriguing, it may be possible to probe the electronic structure of the first layer of metal

atoms in an adsorbate system by using the strong spin polarization[18] which accompanies the GRT. This polarization has its origin in the sensitivity of the resonance: if the scattering potential has any dependence on spin, then the resonance energy will be spin dependent. At a photoelectron energy and scattering angle which corresponds to the GRT resonance, the photoemission intensity will be sensitive to the spin state of the scattering atom.

V. CONCLUSION

We have observed a resonance in the scattering amplitude for S(1s) photoelectrons from Ni atoms and interpreted this resonance as a dip in the Ni atom partial cross section for electron scattering related to the Ramsauer-Townsend effect. This generalized Ramsauer-Townsend effect occurs at a particular energy and angle rather than in the total elastic cross section. We have shown that the resonance energy is sensitive to curved wave corrections and, after including some multiple scattering effects, we have derived the S-Ni bond length of c(2x2)S/Ni(100) from the ARPEFS oscillations from nearest neighbor Ni atoms in the presence of the generalized Ramsauer-Townsend resonance. We find this bond length to be 2.20 Å ± .03 Å corresponding to a S-Ni interplanar distance ($d_\perp$) of 1.32 ± .04 Å.

ACKNOWLEDGEMENTS

This work was supported by the Director, Office of Energy Research, Office of Basic Energy Sciences, Chemical Sciences Division of the U.S. Department of Energy under Contract No. DE-AC03-76SF00098. It was performed at the Stanford Synchrotron Radiation Laboratory, which is supported by the Department of Energy's Office of Basic Energy Sciences.

REFERENCES

1. P.J. Orders and C.S. Fadley, Phys. Rev. B 27, 781 (1983).

2. J.J. Barton, S.W. Robey, and D.A. Shirley, "Theory of Angle-Resolved Photoemission Extended Fine Structure", LBL-19324, and submitted to Phys. Rev. B.

3. A. Liebsch, Phys. Rev. Lett. 32, 1203 (1974).

4. P.A. Lee, Phys. Rev. B 13, 5261 (1976).

5. D.A. Shirley, CR in Solid State Materials Science 10, 373 (1982).

6. S.Y. Tong, and C.H. Li, in Chemistry and Physics of Solid Surface v. III, ed. R. Vanselow and W. England, CRC Press, (1982), p. 287.

7. J.J. Barton, C.C. Bahr, Z. Hussain, S.W. Robey, J.G. Tobin, L.E. Klebanoff, and D.A. Shirley, Phys. Rev. Lett. 51, 272 (1983).

8. J.J. Barton, S.W. Robey, C.C. Bahr, and D.A. Shirley, presented at the First International Conference on the Structure of Surfaces, Berkeley, CA., to be published in the Springer Series in Chemical Physics, 1985.

9. J.J. Barton, C.C. Bahr, S.W. Robey, Z. Hussain, E. Umbach, and D.A. Shirley, LBL-14993, submitted to Phys. Rev. B, and references therein.

10. Z. Hussain, E. Umbach, D.A. Shirley, J. Stöhr, and J. Feldhaus, Nucl. Instrum. Methods 195, 115 (1982).

11. J.J.Barton and D.A. Shirley, "Fourier Analysis of Extended Fine Structure with Autoregressive Prediction", LBL-14758.

12. H. Faxen and J. Holtsmark, Z. Physik 45, 307 (1927).

13. For some elements the generalized Ramsauer Townsend effect occurs between 3 A^{-1} and 12 A^{-1} at 180°. It then appears in the EXAFS

spectrum. B.K. Teo and P.A. Lee, J. Am. Chem. Soc. 101, 2815 (1979).

14. G. Martens, P. Rabe, N. Schwentner, and A. Werner, Phys. Rev. B 17, 1481 (1978).

15. J.J. Barton, C.C. Bahr, Z. Hussain, S.W. Robey, L.E. Klebanoff, and D.A. Shirley, Proceedings for the Brookhaven Conference, Advances in Soft X-ray Science and Technology, S.P.I.E. v. 447, 82 (1984).

16. J.J. Barton and D.A. Shirley, Phys. Rev. B 32, 1892 (1985).

17. M. Sagurton, E.L. Bullock, and C.S. Fadley, Phys. Rev. B 30, 7332 (1984).

18. H.S.W. Massey, E.H.S. Burhop, and H.B. Gilbody, Electronic and Ionic Impact Phenomena, v. 1, 2nd ed., Oxford Univ. Press, London (1969).

FIGURE CAPTIONS

Figure 1. S(1s) ARPEFS oscillations from c(2x2)S/Ni(001) along normal emission ([001]). The experimental kinetic energy scale has been converted to a wavenumber scale using an inner potential of 10.5 eV, and the resulting curve has been interpolated with a numerical spline to an even mesh of 128 points.

Figure 2. Fourier transform magnitudes versus scattering path-length difference for k times the data in Fig. 1. In the lower panel (a), the conventional Fourier transform was applied; the upper panel (b) was obtained with the autoregressive linear prediction method described in ref. 11.

Figure 3. Ni scattering amplitudes calculated in the plane wave limit. Each solid line represents the scattering amplitude for the scattering angle indicated. For each scattering angle the amplitude was calculated for wavenumbers from 5-12$\AA^{-1}$; the labeled tick marks give some indication of the wavenumber scale. The amplitudes are plotted in the complex plane to illustrate the connection between scattering intensity and phase shift. Note that the scattering intensity is nearly zero for θ_j=130° and k≈8$\AA^{-1}$.

Figure 4. Fourier filtered ARPEFS data. The Fourier spectrum from Fig. 2 was zeroed above 5.1Å and backtransformed, the amplitude envelop is also plotted as obtained from the complex backtransformation.

Figure 5. Phase shifts for scattering from Ni. The dashed line shows the phase shift calculated with plane wave theory $\theta_j = 127°$. The dotted line is the phase shift from the experimental curve shown in Fig. 2, where the first two Fourier peaks are backtransformed together. A factor of π for the sign difference between direct and scattered waves caused by the p wave angular distribution has been added to the experimental phase and a nominal 3.56Å path-length difference has been removed. The zero crossing jump in phase occurs too high in wavenumber for the plane wave calculation. Solid lines are curved-wave calculations of the phase shift for the indicated scattering angles.

Figure 6. Multiple-scattering GRT phase jumps. Each panel is labeled by the scattering angle for the Ni nearest neighbors. The dashed lines are phase jumps from the scattering calculation described in the text. The solid lines with circles are experimental phase jumps with geometrical path lengths removed. A phase equal to 3.57k radians was subtracted from both theory and experiment phase functions for comparing the 127.5° ($d_\perp$ = 1.35Å) phases, 3.49k radians from 126.5° ($d_\perp$ = 1.30Å), and 3.41k

radians from 125.4° ($d_{\perp}$ = 1.25Å). As in Fig. 5, a factor of π for (-1) was added to all phase functions; an additional factor of π was added to the 131.4° phase for the purpose of display.

Figure 7. Numerical simulation of the normal emission, S(1s) ARPEFS from c(2x2)S/Ni(001) compared to Fourier filtered experimental data. The theory curves were calculated for all scattering paths less than 5.1 Å; the experimental AR Fourier transform in Fig. 2 was zeroed for frequencies above 5.1 Å and backtransformed to give the solid circles. Over the entire energy range, the frequency of the oscillations clearly matches the theory curve for a S-Ni bond length of 2.19 Å better than the curves for shorter or longer bond lengths.

Figure 8. Geometry search for S-Ni interlayer spacing. Plotted symbols are residuals from the least-squares fit of the numerical simulation curves to the Fourier filtered data. The residual is the unweighted sum of the squared differences between theory and experiment between 100 and 414 eV. The solid triangles give the residual for a fixed theory inner potential of 10.5 eV; the crosses correspond to fits in which the theory inner potential was varied. The solid curve is a parabolic fit to the four triangle points between 1.275 and 1.35 Å; the dashed

curve is a parabolic fit to the four crosses in the same region.

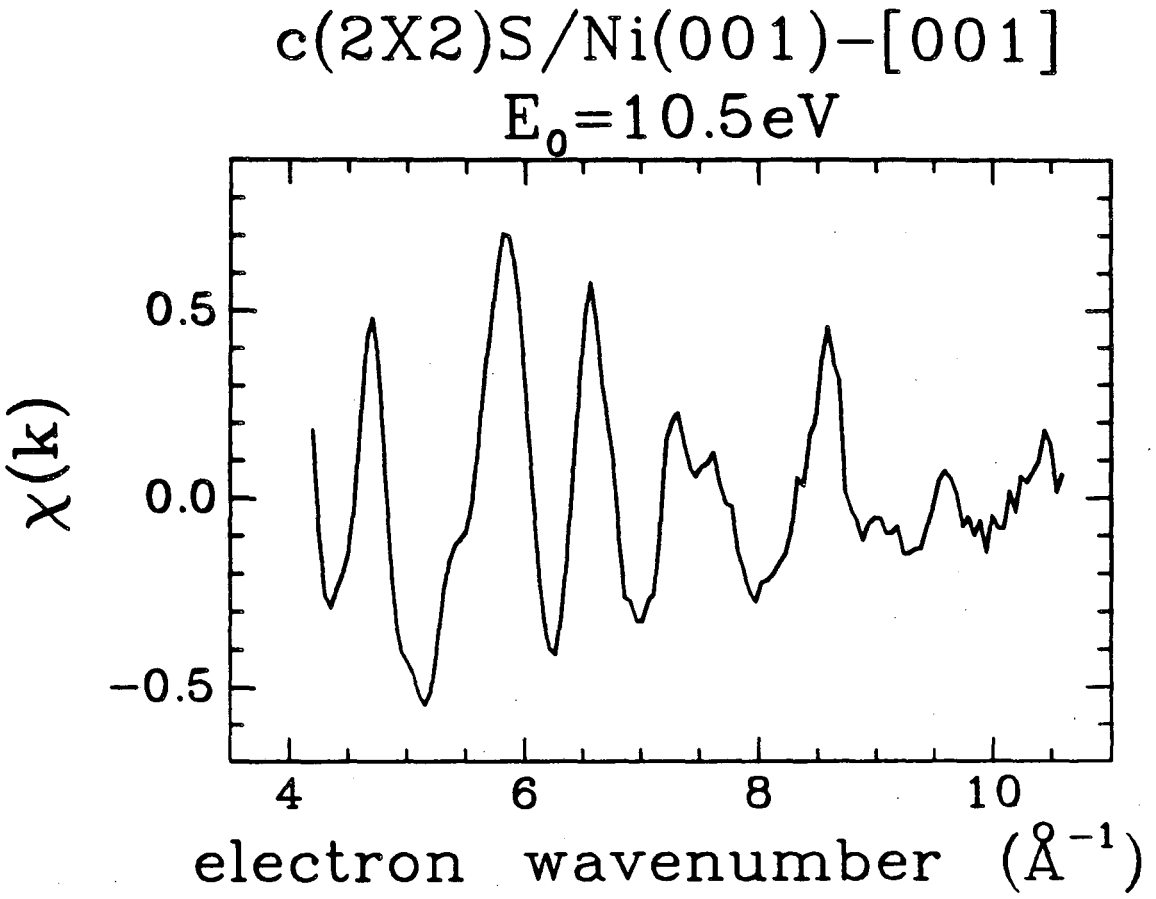

XBL 861-193

Figure 1

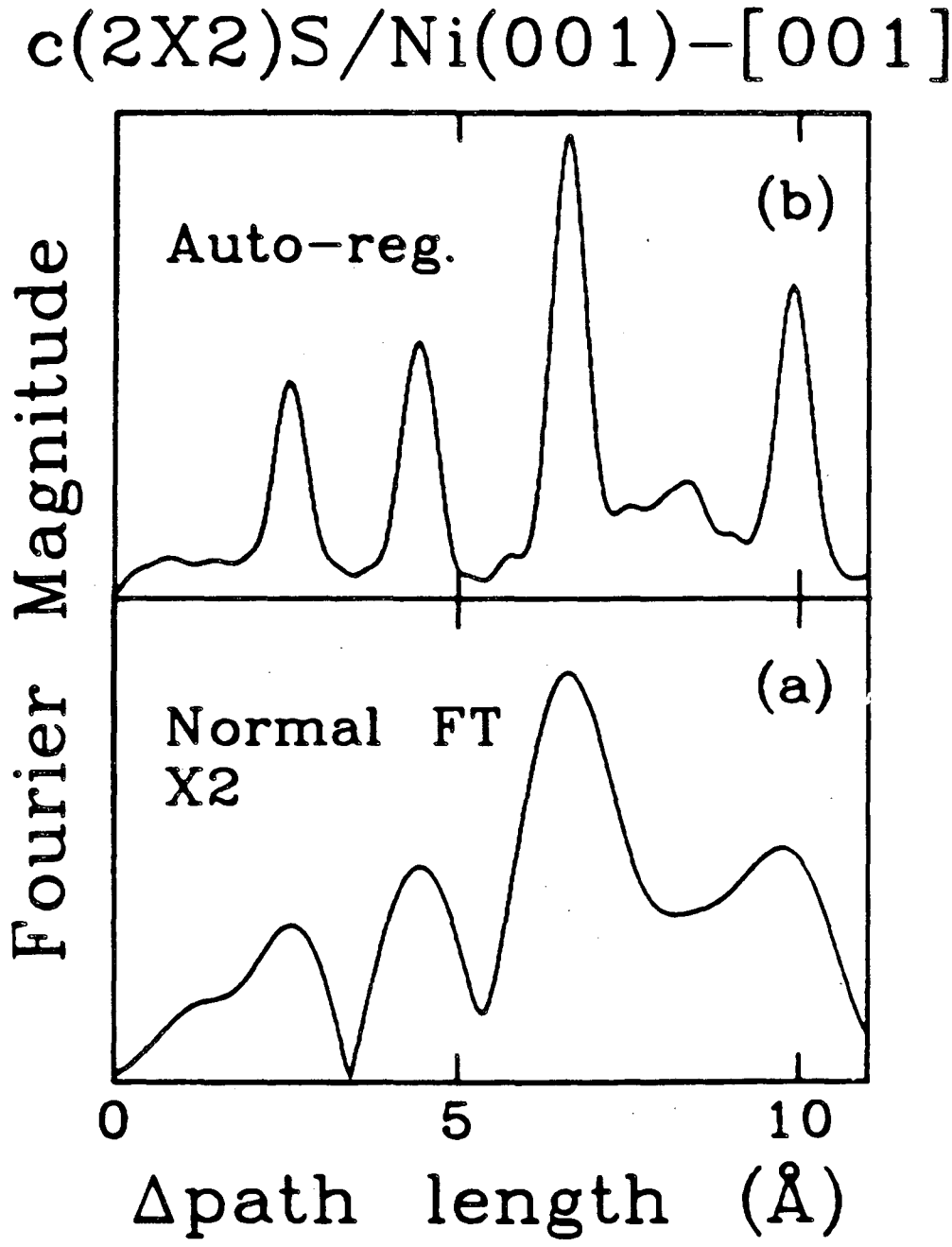

XBL 863-1035

Figure 2

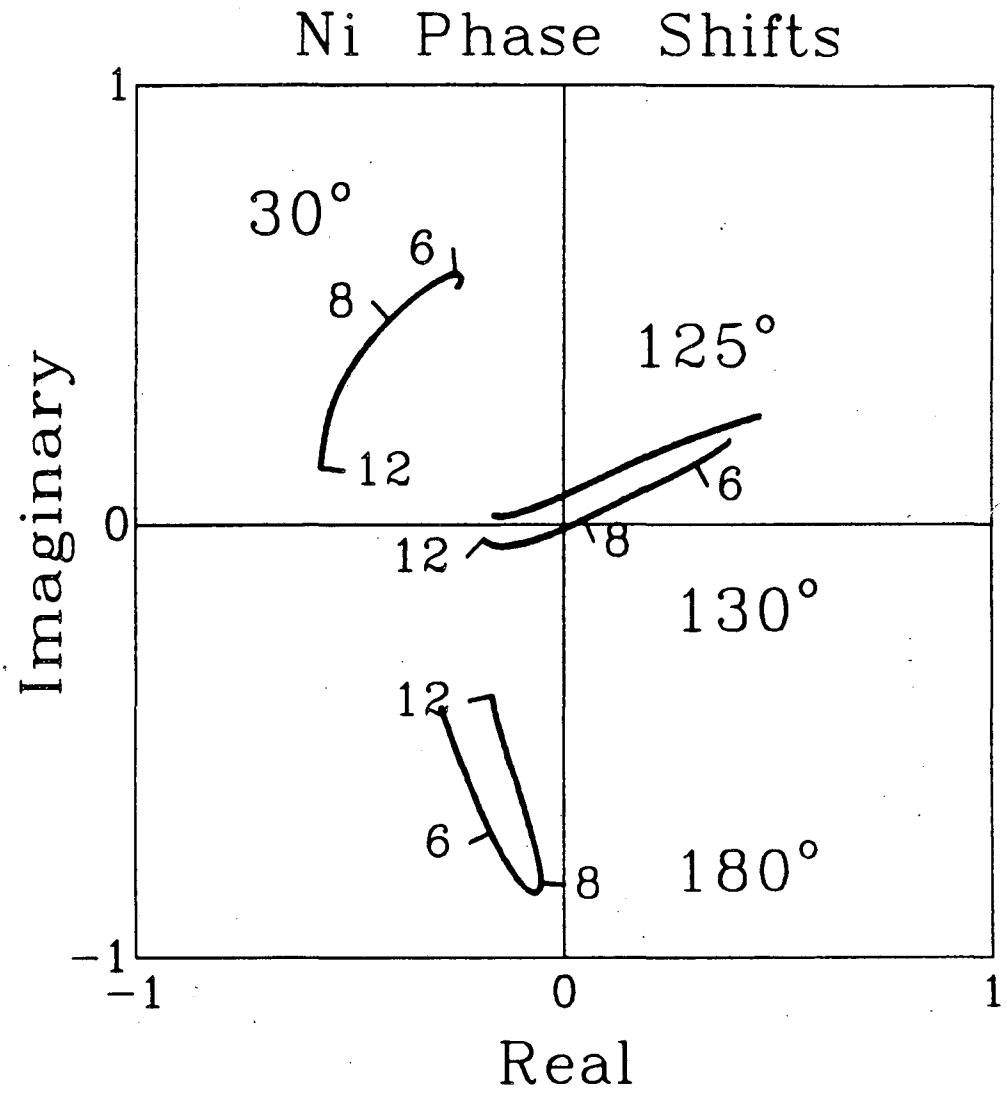

XBL 839-11333

Figure 3

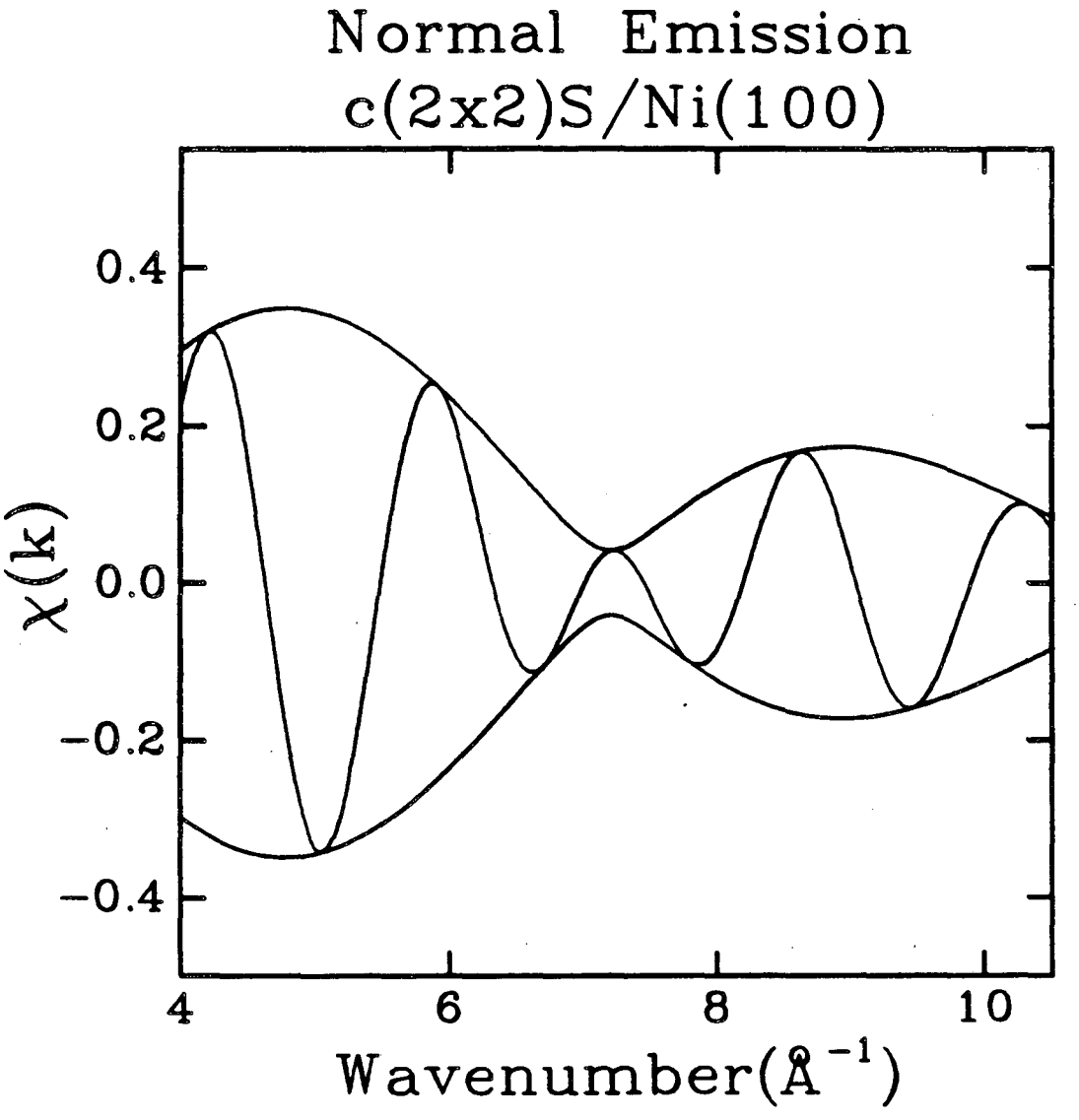

XBL 853-1840

Figure 4

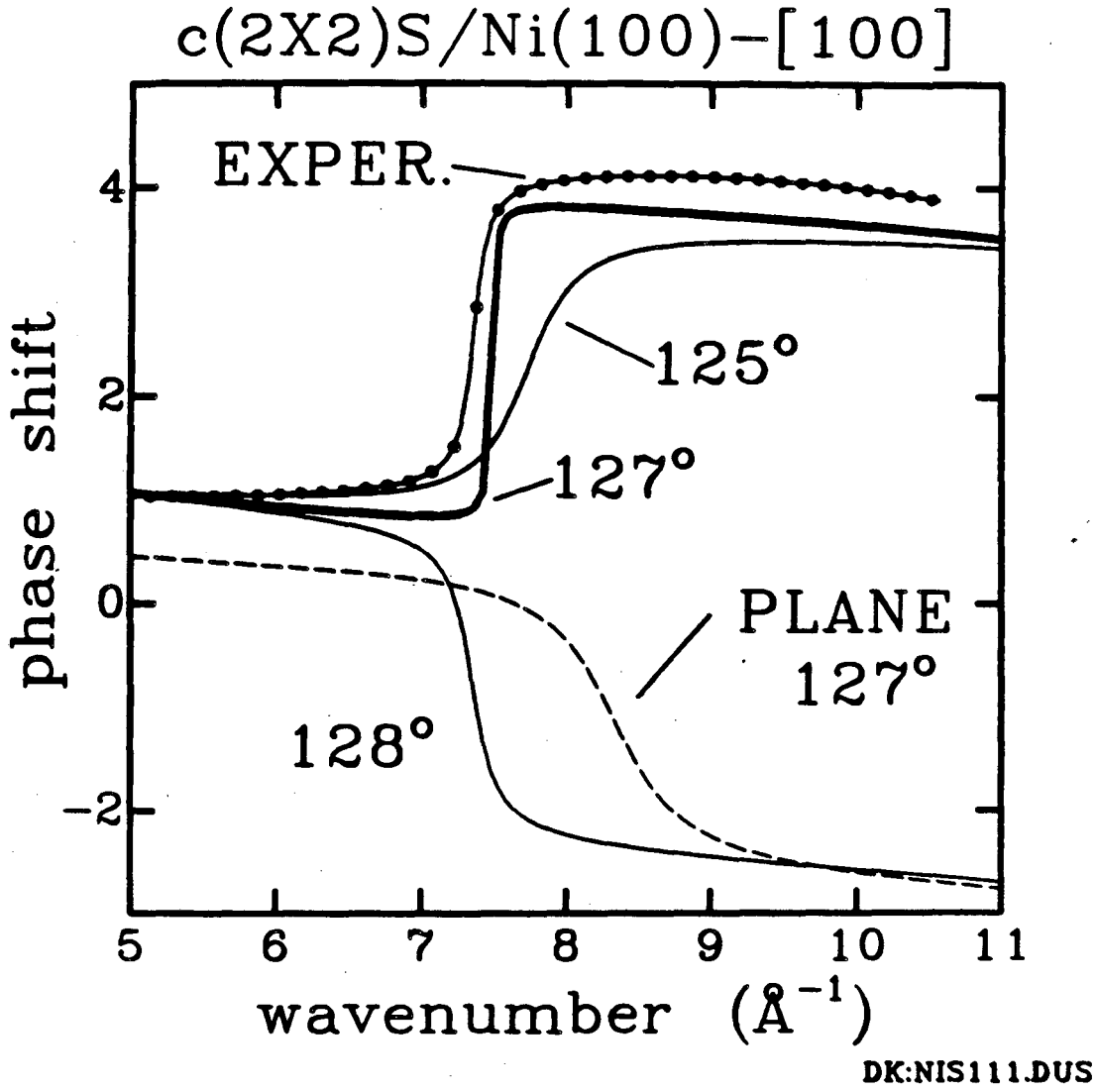

XBL 848-3548

Figure 5

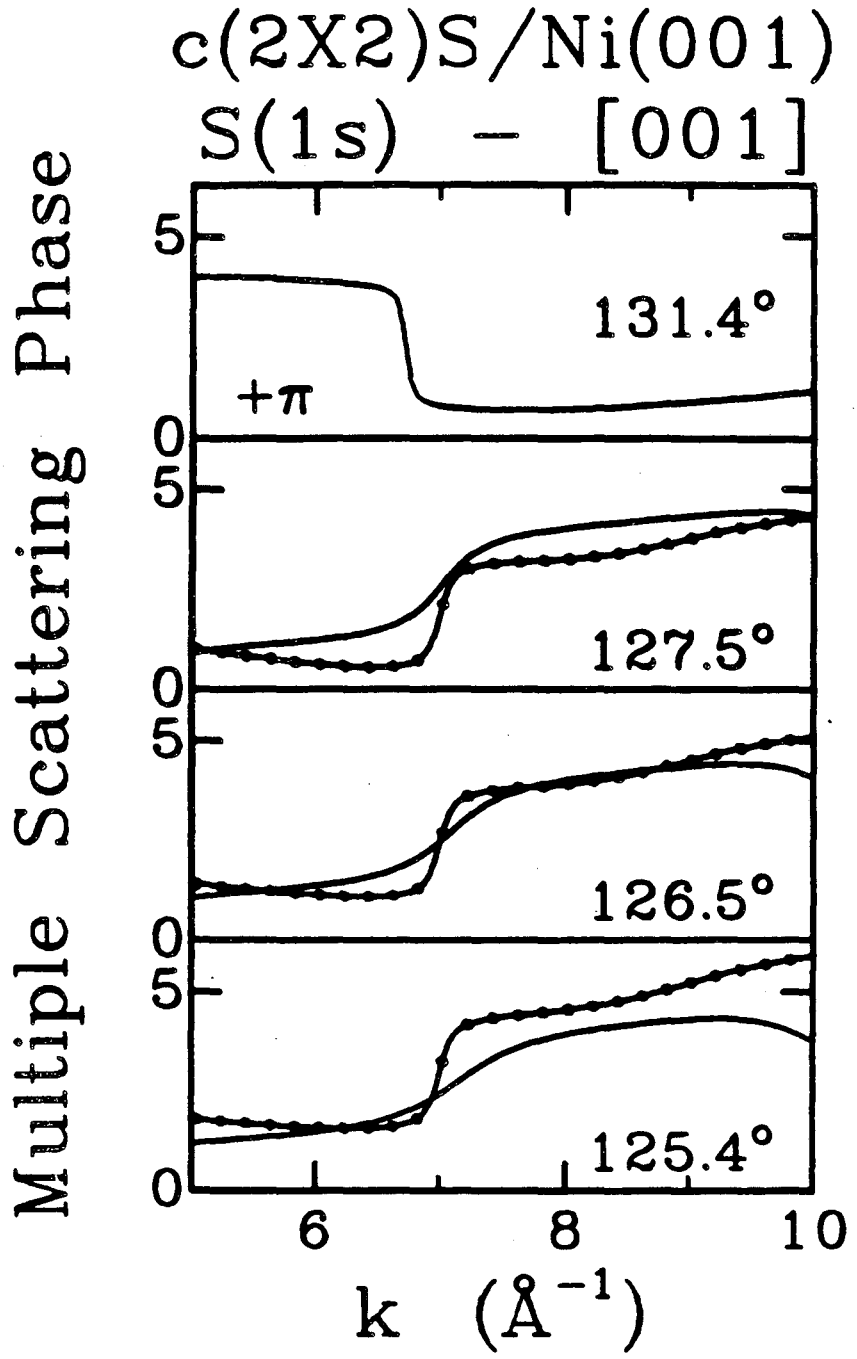

XBL 853-1830

Figure 6

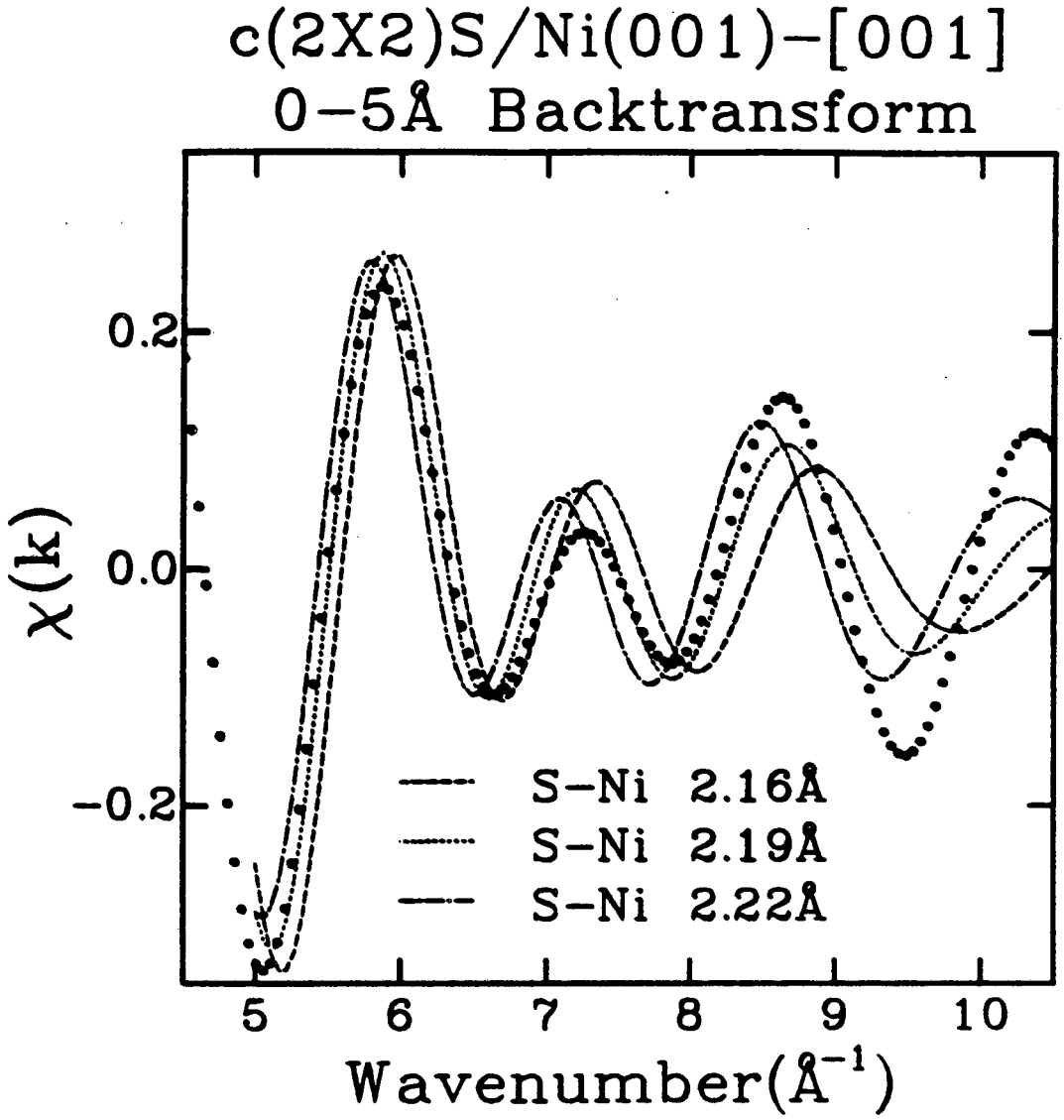

XBL 853-1826

Figure 7

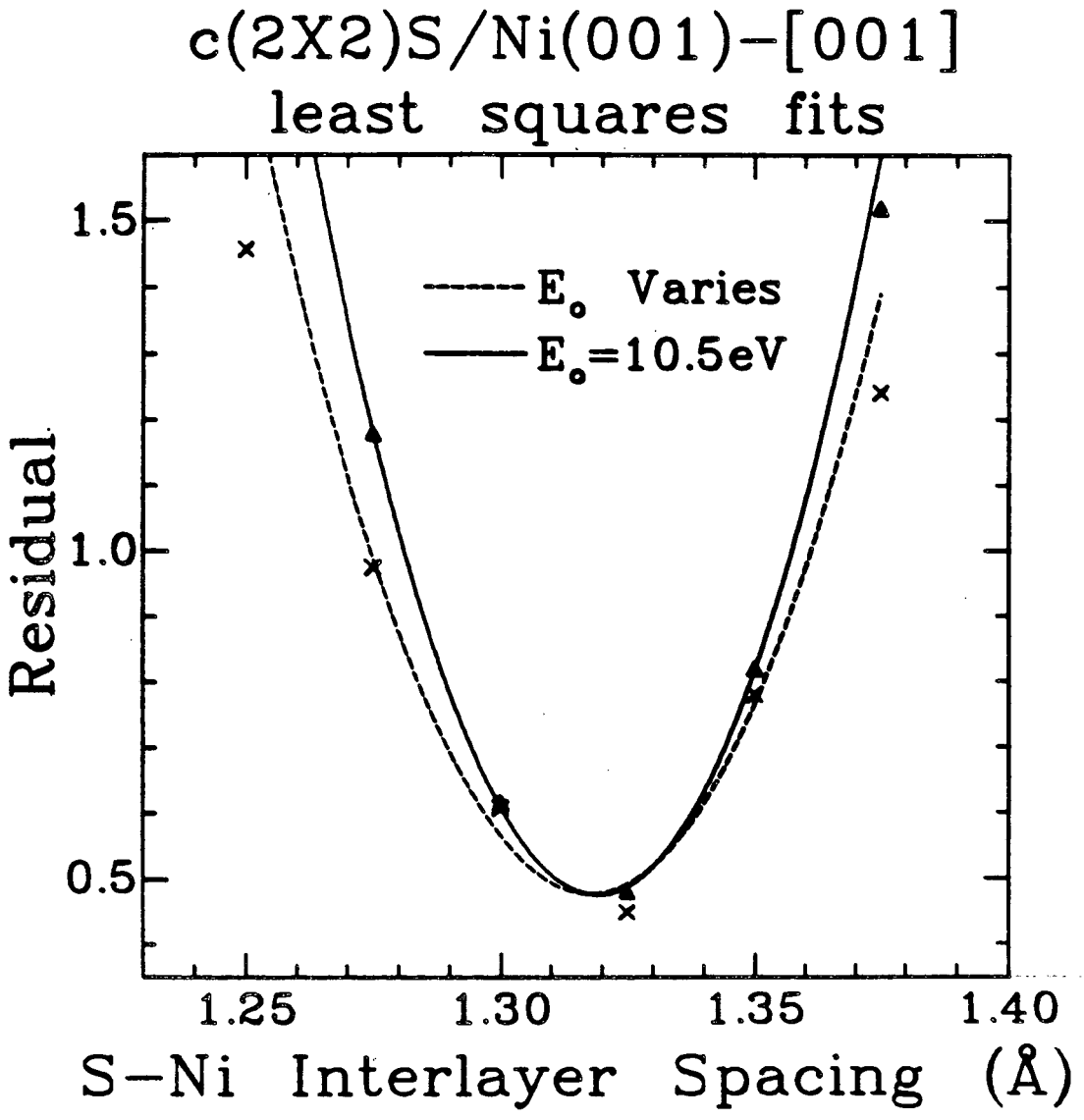

XBL 853-1827

Figure 8

This report was done with support from the Department of Energy. Any conclusions or opinions expressed in this report represent solely those of the author(s) and not necessarily those of The Regents of the University of California, the Lawrence Berkeley Laboratory or the Department of Energy.

Reference to a company or product name does not imply approval or recommendation of the product by the University of California or the U.S. Department of Energy to the exclusion of others that may be suitable.

LAWRENCE BERKELEY LABORATORY
TECHNICAL INFORMATION DEPARTMENT
UNIVERSITY OF CALIFORNIA
BERKELEY, CALIFORNIA 94720